CERIAS Tech Report 2000-05

AN EFFICIENT EDGE EXTRACTION TECHNIQUE USING COLOR COMPONENTS AND MORE POTENTIAL PATTERNS

by Jianping Fan, Walid G. Aref,
A. Rezgui, and Ahmed K. Elmagarmid

Center for Education and Research in
Information Assurance and Security,
Purdue University, West Lafayette, IN 47909

2000-05

An Efficient Edge Extraction Technique Using Color Components and More Potential Patterns

Jianping Fan, Walid G. Aref and A. Rezgui, Amad K. Elmagarmid

Department of Computer Sciences, Purdue University, West Lafayette, IN 47907, USA

ABSTRACT

The edge detection is an useful method for obtaining a simplified image that preserves the domain geometric structures and spatial relationships found in the original image, and it is also the first step for generating the content descriptors for images and videos. The edges in the color images can be classified into two types: (1) The first one is that the respective brightness values of the neighboring pixels are significantly or steadily different; (2) The second one is that the colors for the neighboring pixels are significantly different. This paper presents a more efficient edge extraction algorithm through the integration of three color components, more potential edge patterns and entropy-based feature thresholding. The experimental results have confirmed that this proposed algorithm can provide more reasonable edges than the traditional isotropic edge extraction operators which are only performed on the luminance component of the color images.

Key words: Edge Extraction, Color Components, Thresholding, Edge Patterns, Entropy.

in section 3, where a fast threshold determination algorithm is also proposed. The algorithm for detecting the edges on chrominance components and the fusion rule are introduced in section 4, the experimental results are given in section 5.

2. Color Space and Analysis

Color information has been widely exploited for image segmentation and face-location in recent years[13–17], where the color information is exploited as a feature for partitioning an image into a set of homogeneous regions with similar color and the color information is typically used for region rather than edge segmentation. There have several well-known color space for image representation, display and analysis, thus an image can be presented in a number of different color space models.

RGB: This stands for the three primary colors: *red*, *green* and *blue*. It is a hardware-oriented model and is well known for its color-monitor display purpose because of its easily implementable fashion. However, the *RGB* color model is unable to separate the chrominance components and luminance component efficiently. Moreover, in the *RGB* color space, equal geometric distances do not generally correspond to equal perceptual non-uniformity of the *RGB* color space, thus it is unsuitable for defining the feature metric for color-based image indexing and retrieve, and RGB space is not selected for edge extraction in this paper[18]. Since the *YUV* space is normally used for digital color image storage in the present image and video coding standards, such as JPEG, H.261, H.263 and MPEG, the relationship between the *RGB* space and *YUV* space is

$$\begin{bmatrix} R \\ G \\ B \end{bmatrix} = \begin{bmatrix} 1 & 0 & 1 \\ 1 & -0.194 & -0.509 \\ 1 & 1 & 0 \end{bmatrix} \begin{bmatrix} Y \\ U \\ V \end{bmatrix} \tag{1}$$

CIE(Lab): Colors in the *CIE Lab* space are perceptually more uniformly space than colors are in RGB or HSV spaces, this property of *CIE(Lab)* is very suitable for defining the color distance for image retrieve application and enables the use of a fixed color distance in decision making over a wide range of colors. Moreover, Chroma *ab* have previously been proved to be effective in region-based color image segmentation. In this method, the *YUV* values are first transformed into the *CIE XYZ* values using the formulas.

$$\begin{bmatrix} X \\ Y \\ Z \end{bmatrix} = \begin{bmatrix} 0.982 & 0.167 & 0.518 \\ 1 & 0 & 0 \\ 1.183 & 1.104 & -0.034 \end{bmatrix} \begin{bmatrix} Y \\ U \\ V \end{bmatrix} \tag{2}$$

color images is 4:1:1, four adjacent pixels on luminance component have the same chrominance information.

The luminance component Y of a color image may be taken as a two-dimensional light-intensity function, $I(x, y)$, which contains $(P \times Q)$ pixels, each with a value of brightness, i.e. grey level, from 0 to N. Grey level 0 is the darkest and grey level N is the brightest. In our study, the task of the edge extraction is to classify the pixels into two opposite classes: edge or non-edge, and a second-order neighborhood of current pixel is selected for describing the relationship between current pixel and its neighboring pixels as shown in Fig.1. The edges on luminance component, which are usually defined as the local discontinuities or rapid changes in luminance, may pass the second-order neighborhood with four potential models as shown in Fig.2. Four features, which are used for describing the strength of the edge induced by different edge patterns, are exploited and calculated for detecting the edges of the luminance of the color images, where the weighting coefficients are selected and shown in Fig.3. The first feature, $HOE(m, n)$, which is the absolute difference between its above horizontal neighbors and its below horizontal neighbors of current pixel at (m, n) as shown in Fig.3(a), is termed the strength of the horizontal edge model.

$$\begin{aligned} HOE(m,n) = | \quad & I(m-1,n-1) + 2I(m,n-1) + I(m+1,n-1) - \\ & I(m-1,n+1) - 2I(m,n+1) - I(m+1,n+1)| \end{aligned} \tag{5}$$

where $I(m-1, n-1)$, $I(m, n-1)$, $I(m+1, n-1)$, $I(m-1, n+1)$, $I(m, n+1)$, and $I(m+1, n+1)$ indicate the grey level value of the pixels at $(m-1, n-1)$, $(m, n-1)$, $(m+1, n-1)$, $(m-1, n+1)$, $(m, n+1)$ and $(m+1, n+1)$. $HOE(m, n)$ is used for measuring the strength of edge information on horizontal orientation of current pixel at (m, n).

The second feature, $VOE(m, n)$, which is the absolute difference between its left vertical neighbors and its right vertical neighbors of current pixel at (m, n) as shown in Fig.3(b), is termed the strength of the vertical edge pattern.

$$\begin{aligned} VOE(m,n) = | \quad & I(m-1,n-1) + 2I(m-1,n) + I(m-1,n+1) - \\ & I(m+1,n-1) - 2I(m+1,n) - I(m+1,n+1)| \end{aligned} \tag{6}$$

where $I(m-1, n-1)$, $I(m-1, n)$, $I(m-1, n+1)$, $I(m+1, n-1)$, $I(m+1, n)$, and $I(m+1, n+1)$ indicate the grey level value of the pixels at $(m-1, n-1)$, $(m-1, n)$, $(m-1, n+1)$, $(m+1, n-1)$, $(m+1, n)$ and $(m+1, n+1)$. $VOE(m, n)$ is used for measuring the strength of edge information on vertical orientation of current pixel at (m, n).

The third feature, $NOE(m, n)$, which is the absolute difference between its left-above diagonal neighbors and its right-below diagonal neighbors of current pixel at (m, n) as shown in Fig.3(c), is termed the strength of the northeastern diagonal edge pattern.

$$\begin{aligned} NOE(m,n) = | \quad & 2I(m-1,n-1) + I(m,n-1) + I(m-1,n) - \\ & I(m+1,n) - I(m,n+1) - 2I(m+1,n+1)| \end{aligned} \tag{7}$$

where $I(m-1, n-1)$, $I(m, n-1)$, $I(m-1, n)$, $I(m+1, n)$, $I(m+1, n)$, and $I(m+1, n+1)$ indicate the grey level value of the pixels at $(m-1, n-1)$, $(m, n-1)$, $(m-1, n)$, $(m+1, n)$, $(m, n+1)$ and $(m+1, n+1)$. $NOE(m, n)$ is used for measuring the strength of edge information on northeastern diagonal orientation of current pixel at (m, n).

where f_i is equal to the number of pixels which have the maximum edge strength feature as $i(T+1 \leq i \leq M)$, $\sum_{h=T+1}^{M} f_h$ indicate the total number of pixels which have the maximum edge strength features in range $T+1 \leq i \leq M$. Then the entropies for these two classic regions, non-edge and edge, can further be defined as

$$H_n(T) = -\sum_{i=0}^{T} P_n(i) log P_n(i) \tag{13}$$

$$H_e(T) = -\sum_{i=T+1}^{M} P_e(i) log P_e(i) \tag{14}$$

The global threshold vector $\bar{T}$, which is selected for performing the non-edge and edge pixels classification, has to satisfy the following criterion functions[24–26].

$$H(\bar{T}) = \max_{T=0,1,2,\cdots,M} \{H_n(T) + H_e(T)\} \tag{15}$$

In order to find the global maximum of Eq.(15), the computation burden for the traditional exhaustive searching technique is bounded by $O(M^2)$ because it takes $O(M)$ computation time to obtain the two entropies for each element and there are M potential elements.

3.2. Fast Search Algorithm

For reducing the search burden on determining the global segmentation threshold, an efficient search algorithm is proposed through exploiting the recursive iterations on calculating the probabilities $P_n(i)$, $P_e(i)$ and the entropies $H_n(T)$, $H_e(T)$, where the computation burden is induced by calculating the re-normalized part repeatedly. We first define the total number of the pairs in non-edge region and edge region(the re-normalized parts used in Eqs.(11) and (12)) when the threshold is set to T,

$$P_0(T) = \sum_{h=0}^{T} f_h \tag{16}$$

$$P_1(T) = \sum_{h=T+1}^{M} f_h \tag{17}$$

The corresponding total number of pairs in non-edge and edge regions at global threshold $T+1$ can be calculated as

$$P_0(T+1) = \sum_{h=0}^{T+1} f_h = \sum_{h=0}^{T} f_h + f_{T+1} = P_0(T) + f_{T+1} \tag{18}$$

$$P_1(T+1) = \sum_{h=T+2}^{M} f_h = \sum_{h=T+1}^{M} f_h - f_{T+1} = P_1(T) - f_{T+1} \tag{19}$$

if and only if one of its three color components is detected as the edge and set to 1, otherwise, it is classified as the non-edge pixel and set to 0.

5. Experimental Results

For evaluating the real performance of this proposed edge extraction algorithm, we have tested many images which include very different image components, the results of two CIF images "Akiyo", "Foreman" and three QCIF images "Mother and Daughter", "Salesman" and "Carphone" are shown.

Fig.4(a) shows the original image of "Akiyo", Fig.4(b) is the extracted edges by performing this proposed edge extraction algorithm on three color components, Fig.4(c) is the extracted edges by performing this proposed algorithm only on the luminance component. One can find that this proposed edge extraction algorithm can provide more meaningful results, some obvious edges of the color monitor are missed by the edge extraction procedure which is only based on the luminance information. The experimental results of Prewitt, Sobel, Laplacian and Roberts operators are shown in Fig.4(d), Fig.4(e), Fig.4(f) and Fig.4(g), where the threshold for edge extraction are also determined automatically by this proposed fast entropy algorithm. The extracted human face is shown is Fig.4(h), the white regions, which are in the inside of the human face, are the extracted eyes, mouth and nose.

Fig.5(a) shows the original image of "Foreman", Fig.5(b) is the extracted edges of the image by performing this proposed edge extraction algorithm on three color components. Fig.5(c) is the obtained edge information by performing this proposed edge extraction algorithm only on the luminance component. One can also find that this proposed edge extraction algorithm, which is performed on three color components, can provide more details because some parts of the human hat edge is missed if the edge extraction procedure is only performed on the luminance component. The experimental results of Prewitt, Sobel, Laplacian and Roberts operators, which perform the edge extraction procedure only on the luminance component, are shown in Fig.5(d), Fig.5(e), Fig.5(f) and Fig.5(g). The extracted human face is shown in Fig.5(h).

Fig.6(a) shows the original image of "Mother and Daughter", Fig.6(b) is the extracted edges of the image by this proposed algorithm. The experimental results of Prewitt, Sobel, Laplacian and Roberts operators are shown in Fig.6(c), Fig.6(d), Fig.6(e) and Fig.6(f), one can find that this proposed algorithm can provide more meaningful results and its performance is not depended on the image format. Fig.7(a) shows the original image of "Salesman", Fig.7(b) is the extracted edges of the image by this proposed algorithm. The corresponding experimental results of Prewitt, Sobel, Laplacian and Roberts operators are shown in Fig.7(c), Fig.7(d), Fig.7(e) and Fig.7(f). Fig.8(a) shows the original image of "Carphone", Fig.8(b) is the extracted edges of the image by this proposed algorithm. The experimental results of Prewitt, Sobel, Laplacian and Roberts operators are shown in Fig.8(c), Fig.8(d), Fig.8(e) and Fig.8(f). The extracted human face is shown in Fig.8(h).

6. Conclusion

A fast edge extraction algorithm is proposed, where three color components, fast entropic thresholding algorithm and more potential edge patterns are integrated for obtaining more reasonable

References

[1] L. Davis, "Survey of edge detection techniques", Computer Vision, Graphics and Image Process. **4**, 248-270(1975).

[2] N. Pal and S. Pal, "A Review on image segmentation techniques", Pattern Recognition **26**, 1277-1294(1993).

[3] J. Prewitt, "Object enhancement and extraction", in Picture Processing and Psychopictures, B. Lipkin and A. Rosenfeld, Eds. New Yok: Academic, 1970.

[4] L.G. Roberts, "Machine perception of three-dimensional solids", in Optical and Eletrooptical Information Processing, J.T. Tripperts et al., Eds. Cambridge, MA: MIT Press, 1965.

[5] A. Rosenfeld and A.C. Kak, Digital Image Processing, 2nd ed. New York, Acedemic, 1982.

[6] D. Marr and E. Hildreth, "Theory of edge detection", Proc. Roy. Soc. Londan B **207**, 187-217(1980).

[7] R. Haralick, "Digital step edges from zero crossing of second directional derivatives", IEEE Trans. Pattern Anal. Mach. Intell. **6**, 58-68(1984).

[8] J. Canny, "A computational appraoch to edge detection", IEEE Trans. Pattern Anal. and Mach. Intell. **8**, 679-698(1986).

[9] E. Hildreth, "The detection of intensity changes by computer and biological vision systems", Compter Vision, Graphics and Image Process. **22**, 1-27(1983).

[10] M.J. Swain and D.H. Ballard, "Color Indexing", Internat. J. Computer Vision **7**, 11-32(1991).

[11] Y. Gong and M. Sakauchi, "Detection of regions matching specified chromatic features", Computer Vision and Image Understanding **61**, 263-269(1995).

[12] Y. Ohta, T. Kanade and T. Sakai, "Color information for region segmentation", Computer Grahpics Image Processing **8**, 313-333(1978).

[13] G. Wei and I.K. Sathi, "Face detection for image annotation", Pattern Recognition Letters **20**, 1313-1321(1999).

[14] D. Chai and K.N. Ngan, "Face segmentation using skin-color map in videophone applications", IEEE Trans. on Circuits and Systems for Video Technology **9**, 551-564(1999).

[15] J. Cai and A. Goshtasby, "Detecting human faces in color images", Image and Vision Computing **18**, 63-75(1999).

[16] Y. Dai, Y. Nakano, "Face-texture model based on SGLD and its applications in face detection in a color scene", Pattern Recognition **29**, 1007-1017(1996).

[17] M. Reinders, P. Beek, B. Sankur and J. Lubbe, "Facial feature localization and adaptation of a generic face model for model-based coding", Signal Processing: Image Communication **7**, 57-74(1995).

Figure Captions

- Fig.1: The second-order neighborhood of current pixel.
- Fig.2: The selected edge patterns: (a) horizontal edge model; (b) vertical edge model; (d) northeastern diagonal edge model; (c) northwestern diagonal edge model.
- Fig.3: The coefficients of the edge patterns: (a) horizontal edge model; (b) vertical edge model; (d) northeastern diagonal edge model; (c) northwestern diagonal edge model.
- Fig.4: (a) the original image of "Akiyo"; (b) the extracted edges by performing the proposed edge extraction algorithm on three color components; (c) the extracted edges by performing the proposed algorithm only on the luminance component;(d) the corresponding edges extracted by Prewitt operator; (e)the corresponding edges extracted by Sobel operator; (f) the edges extracted by Laplacian operator; (g) the edges extracted by Roberts operator; (h) the extracted human face.
- Fig.5: (a) the original image of "Foreman"; (b) the extracted edges by performing the proposed algorithm on three color components; (c) the extracted edges by performing the proposed algorithm only on the luminance component; (d) the corresponding edges extracted by Prewitt operator; (e)the corresponding edges extracted by Sobel operator; (f) the edges extracted by Laplacian operator; (g) the edges extracted by Roberts operator; (h) the extracted human face.
- Fig.6: (a) the original image of "Mother and Daughter"; (b) the extracted edges by the proposed algorithm; (c) the corresponding edges extracted by Prewitt operator; (d) the corresponding edges extracted by Sobel operator; (e) the edges extracted by Laplacian operator; (f) the edges extracted by Roberts operator.
- Fig.7: (a) the original image of "Salesman"; (b) the extracted edges by the proposed algorithm; (c) the corresponding edges extracted by Prewitt operator; (d)the corresponding edges extracted by Sobel operator; (e) the edges extracted by Laplacian operator; (f) the edges extracted by Roberts operator.
- Fig.8: (a) the original image of "Carphone"; (b) the extracted edges by the proposed algorithm; (c) the corresponding edges extracted by Prewitt operator; (d)the corresponding edges extracted by Sobel operator; (e) the edges extracted by Laplacian operator; (f) the edges extracted by Roberts operator; (g) the extracted human face.

① Edge Extraction and Comparision

(a)

(b)

(c)

(d)

(e)

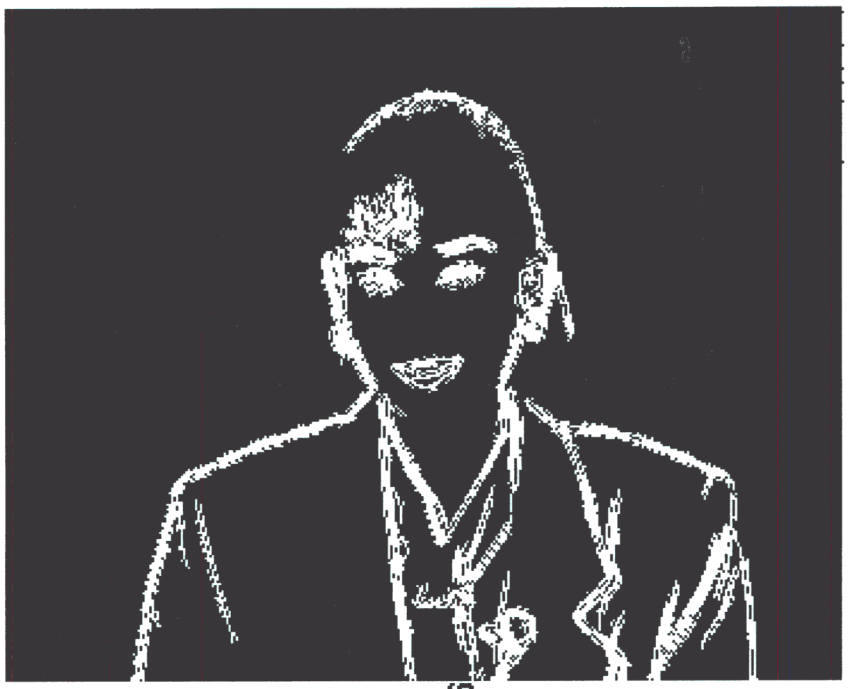

(f)

(g)

(h)

(a)

(b)

(c)

(d)

(e)

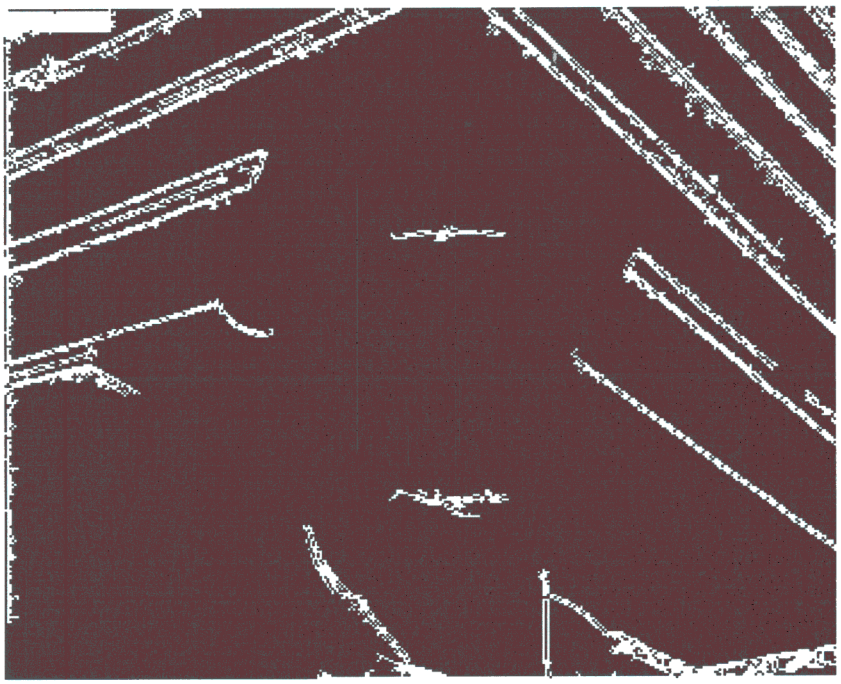

(f)

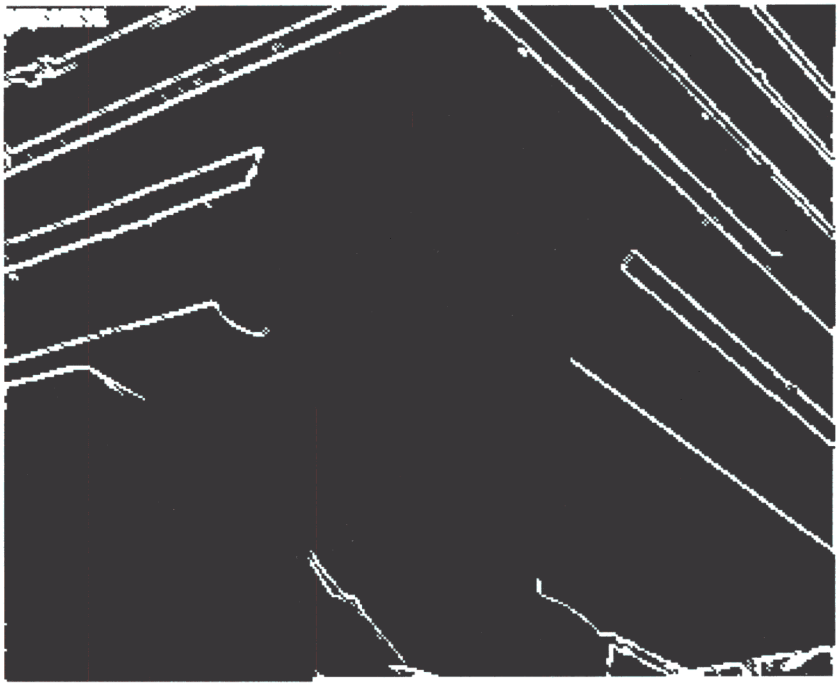

(g)

(h)

(a)

(b)

(c)

(d)

(e)

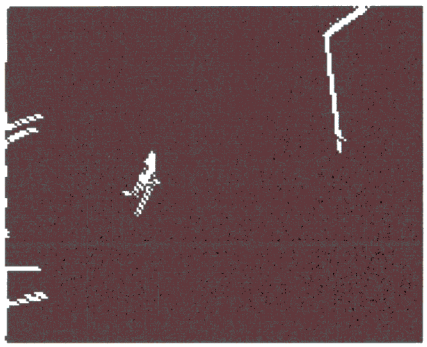

(f)

(a)

(b)

(c)

(d)

(e)

(f)

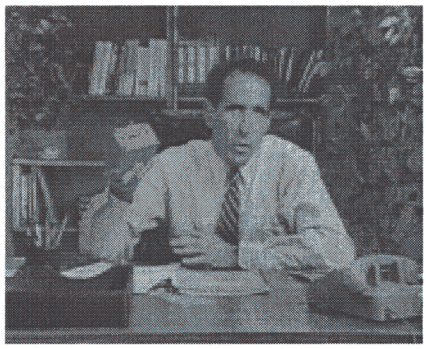

(a)

(b)

(c)

(d)

(e)

(f)